Journal of Hazardous Materials, 30 (1992) 83–95
Elsevier Science Publishers B.V., Amsterdam

An XPS and SEM/EDS characterization of leaching effects on lead- and zinc-doped portland cement

David L. Cocke, M. Yousuf A. Mollah, J.R. Parga, Thomas R. Hess and J. Dale Ortego

Environmental Chemistry Laboratory, Department of Chemistry, Lamar University, Beaumont, TX 77710 (USA)

(Received May 13, 1991; accepted September 10, 1991)

Abstract

The characterization of leaching effects on portland cement doped with lead and zinc has been carried out by X-ray photoelectron spectroscopy (XPS) and scanning electron microscopy/energy dispersive spectroscopy (SEM/EDS). Evidence is presented from XPS and SEM/EDS results that the dopant metal ions are preferentially adsorbed on the surface of the cementitious materials. Leaching tests reveal that most of the Zn^{2+} ions and some of the Pb^{2+} ions are dissolved. A chemical shift with respect to the Si(2*p*) XPS peak occurs due to the increased polymerization of the silicates present in cement. The distribution of the cations before and after leaching is discussed in relation to the XPS and SEM/EDS results.

1. Introduction

Solidification/stabilization (S/S) of hazardous industrial waste has been used for more than two decades. This technology uses selected materials such as portland cement, fly-ash, pozzolan, lime, etc., for binding the hazardous waste prior to landfilling. Although the application of S/S technology has been widely used, there remains a lack of fundamental understanding of the physical and chemical changes that take place as a result of solidification of the priority pollutants metals (Cr, Pb, Ba, Se, Zn, Ag, Hg, As and Cd). Little is known about: (a) the adsorption behaviors of different metal cations on cementitious materials, (b) the chemical and physical changes that take place as a result of adsorption of these metal ions, (c) the effect on cement structure by solidification, and (d) the leaching behavior of different metal cations adsorbed on these substances. In recent publications [1–8], we have shown how modern

Correspondence to: Dr. D.L. Cocke, Environmental Chemistry Laboratory, Department of Chemistry, Lamar University, Beaumont, TX 77710 (USA).
[a]Visiting Professor, Department of Chemistry, University of Dhaka, Bangladesh.
[b]Visiting Professor, C. Graduados, Tec. Saltillo, Mexico.

0304-3894/92/$05.00

surface analysis techniques (X-ray photoelectron spectroscopy (XPS), Auger electron spectroscopy (AES), ion scattering spectroscopy (ISS), etc.), bulk characterization techniques (X-ray diffractometry (XRD), scanning electron microscopy (SEM), energy dispersive X-ray spectroscopy (EDS), etc.), and optical spectroscopies (FTIR, solid state NMR, etc.) can be successfully utilized to reveal the chemistry and leaching mechanisms of the S/S process.

High resolution solid state ^{29}Si NMR techniques have been successfully applied to characterize the hydration products of portland cement [9–11]. The chemical shift of ^{29}Si nuclei in various silica minerals is dependent on the nature of the X group in Si–O–X units [12]. This chemical shift has been successfully used to characterize the nature of silicate polymers in hydrated cements [13]. Ortego et al. [14] have reported, via FTIR and ^{29}Si NMR studies of lead- and zinc-doped portland cement, that silicon polymerization during hydration is slightly enhanced with lead doping, while being retarded in the presence of zinc.

Today, XPS is widely used in surface characterization because it probes the surface core-level electronic states, thus providing qualitative and semi-quantitative information concerning the surface. Shifts in the core-level electronic states provide information concerning the chemical state of the surface components as well as knowledge of the bonding interactions between these components. In recent publications [15–17], we have demonstrated how this surface analysis technique can be used in elucidating the binding and chemical environment in clay, clay minerals and other Si-containing compounds. The position of Si(2*p*) core electronic states in the silicate minerals has been found to be a diagnostic test for delineating the surface conditions in these substances [18, 19]. Carriere et al. [19] have carried out extensive studies of the Si(2*p*) XPS peaks in Si-containing minerals. Based on the Si(2*p*) peak positions they have grouped these substances into four categories: (1) elemental silicon at a binding energy (*BE*) of 99.0 eV, (2) Fe–Si alloys at $BE = 100.0$ eV, (3) intermediate Si oxidation states or those silicate minerals containing less than four Si–O bonds per Si atom at $BE = 102.0$–103.0 eV and (4) heavily oxidized Si-containing minerals that contain SiO_4 tetrahedra linked at four corners by–Si–O–Si–bonds at $BE = 104.0$ eV.

We have reported [1] via XPS and ISS studies of lead- and chromium-doped portland cement that lead is located primarily on the outer surface of the cement matrix while chromium is dispersed in the bulk. XPS and ISS results combined with SEM data indicated that lead is associated with the tricalcium silicate (C_3S) and the β-dicalcium silicate (β-C_2S) components of the cement matrix. We have also found [2] from XPS and FTIR studies of cement doped with barium nitrate, that the presence of Ba^{2+} cations in the cement matrix enhances the polymerization of orthosilicate units in cement. Portland cement doped with mercury has also been investigated using XPS and EDS techniques [3]. The results indicate that mercury does not form a surface complex with

the cement matrix, but is present as the polymeric yellow form of mercuric oxide. In a continuation of our previous works, we report here some XPS and SEM/EDS studies of both leached and unleached samples of lead and zinc-doped portland cement.

2. Experimental

Portland cement, Type 1, was used to prepare the samples. Standard solutions of 10.0 wt% lead and zinc nitrates were prepared using cation-free water. The solution was then slowly added to the cement while stirring continuously with a mechanical stirrer. A cement/water ratio of 0.40 was maintained in all cases. The doped samples were allowed to set for a period of 28 days at room temperature in air at about 85% relative humidity. One sample of lead and zinc-doped cement was subjected to the TCLP (toxicity characteristic leaching procedure) tests [20] using acetic acid and sodium acetate buffer (pH 4.85) for 2 hours to investigate the leaching characterstics. The samples were stored in air prior to analysis.

Prior to XPS analysis, the samples were vacuum dried. After drying, a portion of the bulk unleached samples (outer surface of the leached sample) was ground into a fine powder and pressed into a stainless steel sample holder. The XPS analysis was carried out using a Kratos XSAM 800 photoelectron spectrometer fitted to a custom-built vacuum chamber. The analysis chamber was maintained at 5×10^{-8} torr or better during the analysis. Magnesium K_α radiation (1253.6 eV) was employed throughout the experiment. The spectrometer, controlled by a DS800 operating system, as operated at low magnification, medium resolution and fixed analyzer transmission (FAT) mode. To compensate for the shift in energy due to surface charging, the observed binding energies were all adjusted by assigning the value for the C(1*s*) line from adventitious carbon to a $BE=285.0$ eV. The C(1*s*) region showed three partially overlapping peaks that in some cases required decomposition and fitting to assign the adventitious carbon peak at 285.0 eV. A low binding energy peak was obtained from the metal sample holder and gave direct information on the electrical connection between the nonconductive sample and the spectrometer. An additional surface charging that uniformly affected all the other observed peaks was accounted for using the middle carbon peak. The high binding energy carbon peak corresponds to carbonate. Samples were run several times until consistent binding energies were obtained for all peaks as compared to our laboratory standards and to the literature.

Prior to SEM/EDS analysis, both leached and unleached samples were dry-cut using an Isomet low speed saw with a diamond studded blade. The sample slices were mounted using double-sided tape and analyzed by a JEOL-6400 scanning electron microscope (SEM) equipped with a Tracor-Northern Series 2 EDS system with a germanium detector and diamond window.

3. Results

The zinc and lead samples were analyzed using XPS and SEM/EDS to determine the extent of the chemical changes that occur upon leaching. The SEM/EDS provides information concerning the morphological and compositional changes that occur upon leaching. The chemical state of the sample constituents and their composition can be delineated from XPS studies. Together, these two techniques are expected to provide better insight into the leaching mechanisms of the solidified wastes.

3.1 XPS results

The photoelectrons and Auger lines indicate the presence of calcium, silicon, carbon, oxygen and lead in the unleached and leached lead samples. The zinc-doped sample contains calcium, silicon, carbon and oxygen in the leached and unleached samples. Zinc was found in the unleached sample only. Only a trace amount of potassium, sulfur and aluminum were detected in both the leached and unleached lead and zinc samples. The binding energies of the major components are given in Table 1. The change in binding energy between leached and unleached samples ($\Delta BE = BE_{\text{leached}} - BE_{\text{unleached}}$) is also given.

The binding energies of the oxygen 1s peaks in the lead and zinc unleached and leached samples occur at about 531.5 and 532.5 eV, respectively. Therefore, a shift (see Fig. 1) in the binding energy of the O(1*s*) peak of about 1 eV occurs. The O(1*s*) binding energy is dependent on the surrounding chemical environment in the cement.

An O(1*s*) binding energy of approximately 531.0–531.5 eV is considered to

TABLE 1

Binding energies (eV) of the major surface components identified in 10.0% lead and 10.0% zinc-doped portland cement

Components Identified	Binding energies (eV)					
	10.0% Pb-doped			10.0% Zn-doped		
	Unleached	Leached	ΔBE	Unleached	Leached	ΔBE
Ca($2p_{3/2}$)	347.1	348.1	1.0	347.0	347.4	0.4
Si(2*p*)	101.2	102.7	1.5	101.0	102.6	1.6
Pb($4f_{7/2}$)	138.4	138.8	0.4	—	—	—
Zn($2p_{3/2}$)	—	—	—	1021.5	—[a]	—[a]
O(1*s*)	531.4	532.5	1.1	531.6	532.4	0.8
C(1*s*)	285.0	285.0	0.0	285.0	285.0	0.0

[a]No zinc was detected.

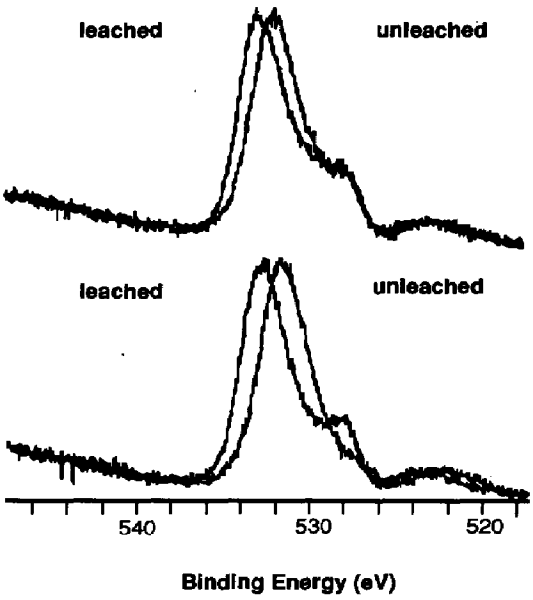

Fig. 1. XPS spectra of O(1*s*) lines for (a) zinc-doped cement, and (b) lead-doped cement.

be characteristic of the O^{2-} oxidation state for hydroxyl, carbonate and silicate anion species in a cement matrix [1, 21, 22]. Although it is rather difficult to use the O(1*s*) peak to infer the chemical state of the oxygen species on the cement surface, the O(1*s*) peak has sometimes been used to differentiate between bridging (–Si–O–Si–) and non-bridging (–Si–O–*X*–, where *X*=Na, Al, Fe, etc.) oxygen atoms in minerals and ceramics [19]. A shift to higher binding energies due to leaching is perhaps indicative of the oxygen reacting with the silicon to form a bridging moiety in the cement matrix.

XPS spectra of Si(2*p*) lines for leached and unleached samples are shown in Fig. 2(a) for zinc-doped cement and in Fig. 2(b) for the lead-doped sample. The peaks appear at 101.2 and 102.7 eV for the unleached and leached lead-doped samples and the corresponding peaks in the zinc-doped samples appear at 101.0 and 102.6 eV, respectively. The XPS peaks in Si(2*p*) have thus been shifted significantly by about 1.5 eV due to leaching. The Si(2*p*) signal has been used to elucidate the structural nature of silicate minerals [15, 19, 23, 24].

Carriere et al. [19] have shown that the diagnostic Si(2*p*) XPS peaks for a heavily oxidized Si-containing mineral occurs at about 104 eV, while an intermediate Si-oxidation state for these silicate minerals occurs at around 102–103 eV. An increase in the binding energy of the Si(2*p*) peaks in the leached samples is therefore indicative of an increase in the number of Si–O bonds per silicon atom, thus leading to enhanced polymerization of silica present in cement.

The Ca($2p_{3/2}$) and Ca($2p_{1/2}$) peaks in the lead-doped samples appear at

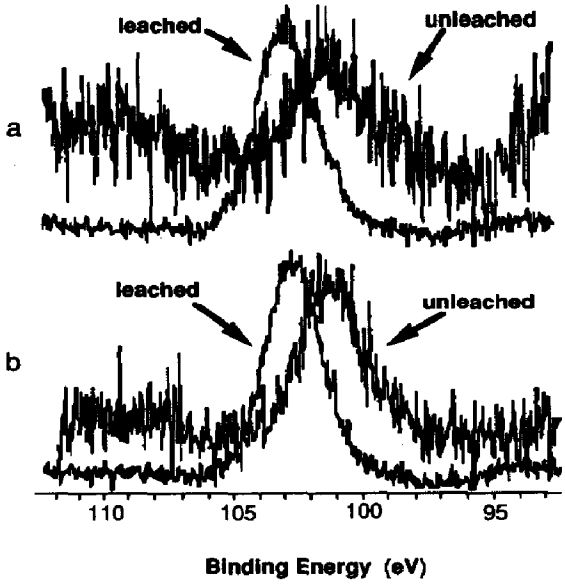

Fig. 2. XPS spectra of (a) zinc-doped cement and (b) lead-doped cement showing shifting of Si(2p) lines due to leaching.

347.1, 350.6 and 348.1, 351.6 eV in the unleached and leached samples, while the corresponding peaks in the zinc-doped spectra appear at 347.0, 350.5 and 347.4, 350.9 eV, respectively. The binding energy difference between the Ca ($2p_{3/2}$) and Ca ($2p_{1/2}$) peaks is about 3.5 eV, which is typical of calcium sulfate, silicate and carbonate [3, 21].

The binding energies of Ca($2p_{3/2}$) peaks in the unleached lead (347.1 eV) and zinc (347.0 eV)-doped samples are similar and approximately equal to the same peak in calcium hydroxide which appears at 346.7 eV (Figs. 3 and 4). It, thus, appears that calcium in hydrated cement is present mostly as calcium hydroxide. This is in agreement with the values reported by Suguma [25] from XPS studies of Ca-based hydrates formed by the interaction of $Ca(OH)_2$ and the chemical constituents present on the surface of ceramic microspheres.

Suguma has reported that the binding energy due to the $2p_{3/2}$ peak appears at 346.7 for $Ca(OH)_2$ and 347.6 and 348.4 eV due to the association of calcium in $CaO–SiO_2–H_2O$ and $CaO–Al_2O_3–SiO_2–H_2O$, respectively. However, the binding energies due to the Ca($2p_{3/2}$) peaks appear at higher positions in the lead (Fig. 3) and zinc-doped (Fig. 4) samples, although the difference between the leached and unleached samples is much more significant for the lead sample (1.0 eV) than the zinc-doped samples (0.4 eV). The reasons for this are not yet known. It does, however, emphasize the difference in surface chemistry between zinc- and lead-doped samples. This difference will be examined in future studies.

The Pb($4f_{7/2}$) peaks in lead-doped samples appear at 138.4 eV for the unleached sample and 138.8 eV for the leached sample (Fig. 5). The relatively

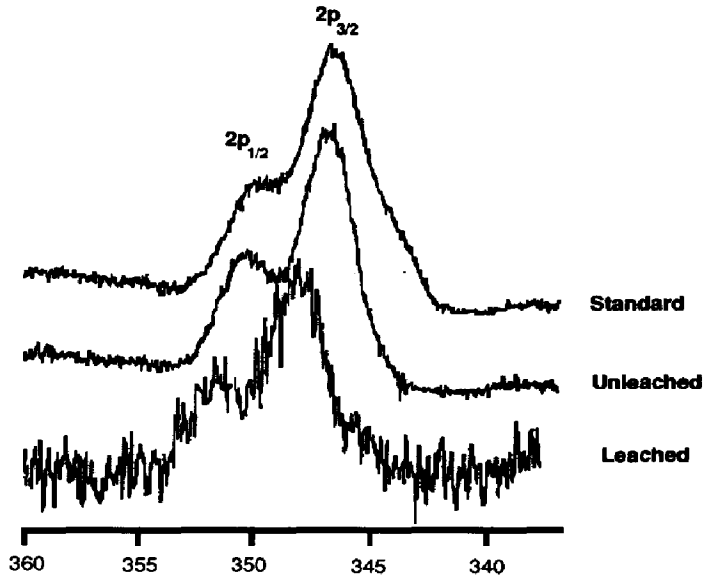

Fig. 3. XPS spectra of Ca $2p_{1/2}$ and Ca $2p_{3/2}$ lines for lead-doped cement and standard $Ca(OH)_2$.

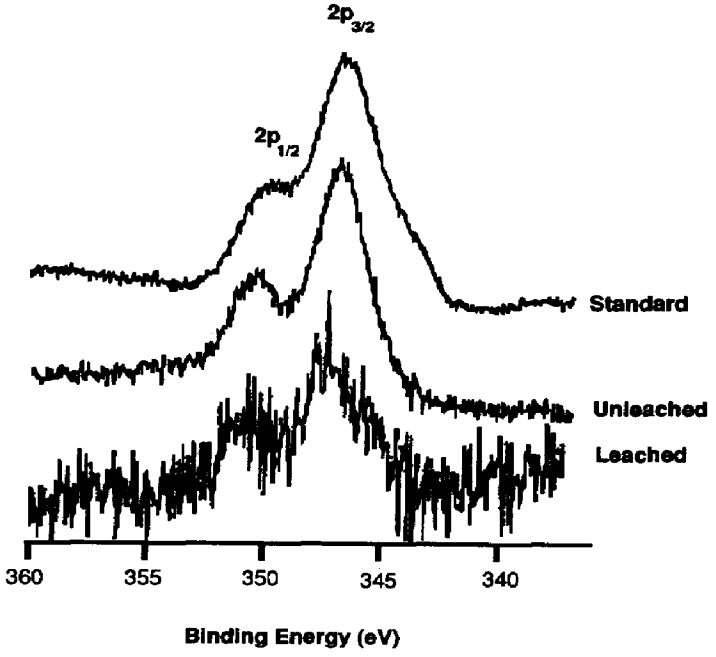

Fig. 4. XPS spectra of $Ca(2p_{1/2})$ and $Ca(2p_{3/2})$ lines for zinc-doped cement and standard $Ca(OH)_2$.

small shift in the binding energy indicates that the chemical state of the lead has not changed significantly upon leaching. The binding energy of the Zn ($2p_{3/2}$) peak appears at 1021.5 eV in the unleached sample. However, no zinc was found in the leached sample indicating that most of the surface zinc has been dissolved during the leaching tests.

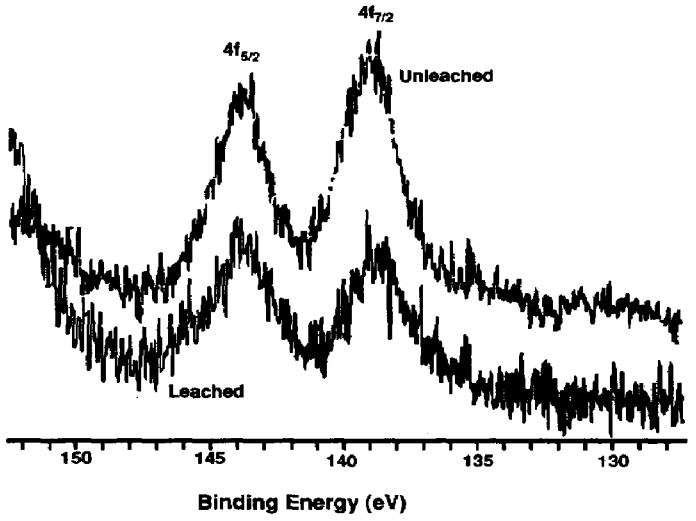

Fig. 5. XPS spectra of lead-doped cement before and after leaching.

3.2 SEM and EDS results

The lead- and zinc-doped samples were also analyzed using scanning electron microscopy (SEM) and energy dispersive spectroscopy (EDS) for qualitative and morphological information of the leached and unleached surfaces.

The SEM micrograph of the unleached side, leached side and unleached and leached front are shown in Fig. 6. The unleached and leached front (Figs. 6b and e) show two distinctive facets of unleached and leached areas. The characteristic morphology of the phases is also quite visible. The inner continuous matrix is similar to the unleached side. The leached sides consist of a "honeycomb" type of structure made up of flakey bright substances. The morphology of the outer leached side may be compared with a cross-linked, poorly crystalline structure and is similar to ettringite commonly present in hydrated cement [26]. The unleached sides (Figs. 6a and d) of both lead- and zinc-doped cement consist of a continuous dark area surrounded by bright flakey material. The zinc-doped cement has more amorphous characteristics than the lead-doped cement, while the lead-doped cement shows more needle-shaped structures. The leached sides (Figs. 6c and f) consist of loosely bound flakey materials with cracks and needle-shaped substances spread over the side. The morphology of the zinc-doped leached sample is fairly similar to the lead-doped leached sample.

The corresponding EDS spectra of the unleached and leached samples are shown in Fig. 7. The following elements have been identified from the lead-doped sample: oxygen, calcium, silicon, aluminum, lead and potassium. It can be seen (Figs. 7a and b) that the concentration of silicon and calcium have been drastically changed due to leaching. The calcium to silicon (Ca/Si) ratio has been considerably reduced in the leached sample due to the dissolution of

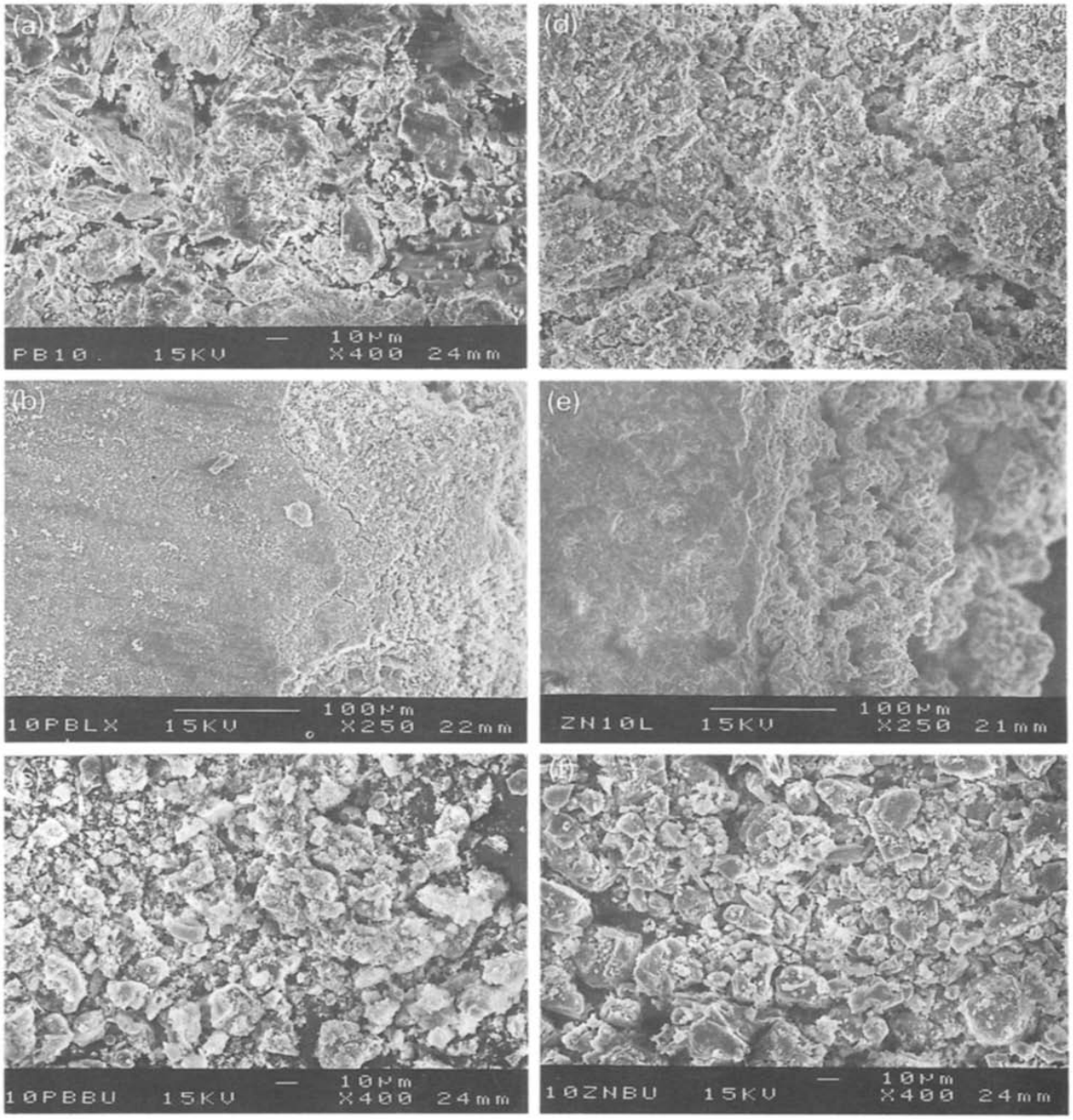

Fig. 6. SEM micrographs of lead (a,b,c)- and zinc (d,e,f)-doped portland cement. (a, d) Unleached samples, (b,e) leached–unleached front, (c,f) fully leached samples.

$Ca(OH)_2$. The concentration of aluminum and potassium has increased slightly as a result of leaching, while the concentration of lead has been decreased.

The elements identified from EDS spectra of the zinc-doped sample include oxygen, calcium, silicon, aluminum and potassium. No zinc or sulfur was detected in the leached sample. It is quite clear (Figs. 7c and d) that the calcium to silicon ratio (Ca/Si) is considerably lower in the leached sample as in the

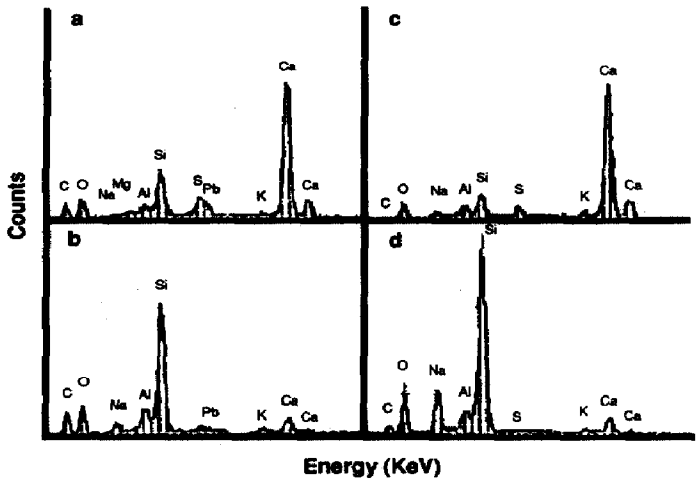

Fig. 7. EDS spectra of lead (a,b)- and zinc (c,d)-doped cement; (a,c) unleached sample, (b,d) leached sample. Note the virtual absence of potassium.

case of the lead-doped cement. These results indicate the presence of higher concentrations of silicon in the near surface regions (1 μm) of the leached sample. The EDS results are compatible with the XPS results presented above.

4. Discussion

The primary objectives of the present work were to (a) investigate the chemistry of leaching, (b) ascertain the positions of the metal dopants in the cement matrix before and after leaching and (c) characterize the environment of silicon in the cement matrix before and after leaching.

The present results confirm previous reports [1] that lead is preferentially adsorbed on the surface of the cementitious material doped with lead and also retardation of the setting of cement by Pb^{2+} ions by blocking the hydration reaction. The binding energy of the Pb(4*f*) XPS peaks indicates the presence of Pb^{2+} ions and is also consistent with silicate, hydroxide and carbonate. The leaching process removes most of the Pb^{2+} ions from the surface of the cement matrix as is evidenced from the much reduced intensity of the Pb(4*f*) XPS peak. The situation is similar for the zinc-doped sample. The presence of flakey materials on the surface of unleached samples and the low intensity of the lead and zinc observed in the EDS support surface binding for both lead and zinc. The SEM micrographs also support this argument.

The binding energy of the Ca($2p_{3/2}$) peaks for the zinc unleached and leached samples are not significantly different and could be attributed to Ca^{2+} in $Ca(OH)_2$. The surface concentration of calcium in the leached samples has been significantly reduced. Since calcium and silicon are the major compo-

nents in portland cement, a rough calculation for comparison purposes of the relative percentage of calcium and silicon in the leached and unleached samples can be made from the EDS spectra after normalization of calcium and silicon peak areas only. In the unleached samples the percentages of silicon and calcium are 29.0 and 71.0 for 10% Pb-doped cement and 19.10 and 80.90 for 10% Zn-doped cement, respectively. The corresponding values in the leached samples are 49.40 and 50.60 for Pb-doped cement and 83.70 and 16.30 for 10% Zn-doped cement. The Ca/Si ratio (2.40 and 1.02 for unleached and leached Pb-doped cement; 4.20 and 0.19 in the unleached and leached Zn-doped cement) thus decreases due to leaching, although the effect is more significant for Zn-doped cement. This is clear evidence that much of the calcium present as calcium hydroxide has been dissolved into the acidic medium. The relative concentration of silicon has been increased due to leaching and loss of hydroxide and sulfate.

The chemical shift with respect to the Si(2*p*) XPS peak is a significant result. McWhinney [21] has reported the *BE* of Si(2*p*) XPS peaks in standard cement, 10% Pb-doped and 10% Zn-doped cement as 101.1, 101.6 and 101.5 eV, respectively. The *BE* of the Si(2*p*) XPS peak in the unleached lead and zinc-doped cement are comparable, while the *BE* of the same peak in the leached sample was found to be 102.7 and 102.6 eV, respectively. The *BE* of the Si(2*p*) peaks have, therefore, been shifted in the leached samples by about 1.5 eV for lead and by 1.6 eV for zinc. The results clearly demonstrate that the silicon environment has undergone drastic changes due to leaching. We have reported [15, 16] via XPS studies that the chemical shift with respect to Si(2*p*) peak can be attributed to the difference in the Si-bonding environment and the BE of the resulting Si-containing compound is dependent on the number of Si–O bonds per Si atom. Calcium silicate hydrate ($CaO \cdot SiO_2 \cdot H_2O$) is the primary cementing and hardening chemical formed on hydration in portland cement and other lime silica systems. It is believed [1] that CaO is a favorable site for acid attack during the leaching process leading to polymerization of the silicates. Ortego et al. [14] have reported, via ^{29}Si NMR and FTIR studies of lead- and zinc-doped cements, that polymerization of the silicates present in the cement matrix occurs due to leaching and the following generalized mechanism of polymerization has been proposed:

$$->Si\text{–}OX + H^+_{(aq)} \longrightarrow ->Si\text{–}OH + X^+_{(aq)} \text{ or}$$

$$>Si\text{–}O_2X + 2H^+_{(aq)} \longrightarrow >Si\text{–}(OH)_2 + X^{2+}_{(aq)}, \text{ etc.}$$

where X = calcium, potassium, sodium or toxic metals ions. Then, condensations via silanol groups produces:

$$Si\text{–}(OH)_x \longrightarrow \text{branched and cross-linked silicates}$$

A *BE* value of 103.0 eV for Si(2*p*) XPS peaks in the leached samples clearly demonstrate that the Si moiety in the cement matrix has been polymerized due to leaching. It is likely that small units of polymerized silica have been linked at one or two corners of O–Si–O tetrahedra. The beehive type morphology present in the leached front support this argument. The presence of trace amounts of potassium in the unleached and leached samples is attributed to the ion exchange mechanism previously reported [1].

5. Conclusions

The XPS and SEM/EDS results confirm previous reports that both zinc and lead are preferentially deposited on the surface of the cement grains. However, the leaching experiments reveal that extended contact of the metal-doped solidified portland cement with the acidic leaching solution attacks and destroys its mineral structures. The leaching solution attacks the calcium silicate hydrate (C–S–H) by removing calcium and dissolving calcium hydroxide from the solidified matrix. This exposes the silicate moiety to the acidic solution leading to increased branching and cross-linking of silicates to produce a crumbly porous solid with very little mechanical strength. The decrease in alkalinity caused by the acidic attack increases the solubility of the hazardous cations as well as undermines the chemical and physical integrity of the cement matrix.

Acknowledgments

The authors gratefully acknowledge partial financial support from the Gulf Coast Hazardous Substance Research Center, Lamar University, Beaumont, Texas and the Robert Welch Foundation, Houston, Texas.

References

1 D.L. Cocke, H.G. McWhinney, D.C. Dufner, B. Horrell and J.D. Ortego, An XPS and EDS investigation of portland cement doped with Pb (II) and Cr (III) cations, Hazard. Waste Hazard. Mater., 6 (3) (1989) 252–267.

2 H.G. McWhinney, M.W. Rowe, D.L. Cocke, J.D. Ortego and G.-S. Yu, X-ray photoelectron and FTIR spectroscopic investigation of cement doped with barium nitrate, Environ. Sci. Health, A25 (5) (1990) 463–477.

3 H.G. McWhinney, D.L. Cocke, K. Blake and J.D. Ortego, An investigation of mercury solidification and stabilization in portland cement using X-ray photoelectron spectroscopy and energy dispersive spectroscopy, Cem. Concr. Res., 20 (1990) 79–91.

4 J.D. Ortego, S. Jackson, G.-S. Yu, H. McWhinney and D.L. Cocke, Solidification of hazardous substances–A TGA and FTIR study of portland cement containing metal nitrates, J. Environ. Sci. Health, 24 (1989) 589–602.

5 H.G. McWhinney, J.D. Ortego and D.L. Cocke, XPS investigation of zinc and cadmium doped portland cement, submitted to Environ. Sci. Health.

6 R. Davis and D.L.Cocke, Analysis of the physical and chemical aspects of leaching behavior in lead and chromium doped portland cement waste forms, Ceram. Trans., 23 (1991) 201.
7 H.G. McWhinney, D.L. Cocke and L. Donaghe, Surface characterization of priority metal pollutants in portland cement, in Proc. HMCRIs 7th Natl. RCRA/Superfund Conf. on Hazardous Waste and Hazardous Materials, St Louis, MO, May 2–4 (1990).
8 M.Y.A. Mollah, J.R. Parga and D.L. Cocke, An infrared spectroscopic examination of cement based solidification/stabilization systems—portland Type V and Type IP with zinc, accepted for Toxic Hazard. Substance Control, 1992.
9 J.R. Barnes, A.D.H. Clague, N.J. Clayden, C.M. Dobson, C.J. Hayes, G.W. Groves and S.A. Rodger, J. Mater. Sci. Lett., 4 (1985) 1293.
10 E. Lippmaa, M. Magi, M. Tarmak, W. Wieker and A.R. Grimmer, Cem. Concr. Res., 12 (1982) 597.
11 N.J. Clayden, C.N. Dobson, C.A. Hayes and S.A. Rodger, J. Chem. Soc., Chem. Commun., 21 (1984) 1396.
12 E. Lippmaa, A.A. Madis, T.J. Penk and G. Engelhardt, J. Am. Chem. Soc., 100 (1978) 1929.
13 F.K. Cartledge, L.G. Butler, D. Chalasani, H.C. Eaton, F.P. Frey, E. Herrera, M.E. Tittlebaum and S.-L. Yag, Environ. Sci. Technol., 24 (1990) 867.
14 J.D. Ortego, Y. Barroeta, F.K. Cartledge and H. Akhter, Environ. Sci. Technol., 25 (1991) 1171.
15 R.K. Vempati, R.H. Loeppert, D.C. Dufner and D.L. Cocke, Soil Sci. Soc. Am. J., 54 (1990) 695.
16 R.K. Vempati, R.H. Loeppert and D.L. Cocke, Solid State Ionics, 38 (1990) 53.
17 R.K. Vempati, D.L. Cocke and J.W. Stucki, X-ray photoelectron spectroscopy of clay and clay minerals. A review article for NATO Book Division, to be published by Reidel, Dordrecht.
18 M.H. Koppleman, in: J.W. Stucki and W.L. Banwart (Eds.), Advanced Chemical Methods for Soil and Clay Minerals, Reidel, Dordrecht, 1980, p. 205.
19 B. Carriere, J.P. Deville, D. Brion and J. Escard, J. Electron Spectrosc. Relat. Phenom., 10 (1977) 85.
20 Federal Register, 51 (1986) 21672–21692 (No. 114, Friday, June 13, 1982).
21 H.G. McWhinney, Surface characterization of priority metal pollutants in portland cement, PhD, dissertation, Texas A & M University, College Station, TX, 1990.
22 D. Briggs and M.P. Seah, Practical Surface Analysis by Auger and X-ray Photoelectron Spectroscopy, Wiley, New York, NY, 1983.
23 S. Hoffman and J.H. Thomas III, J. Vac. Sci. Technol., 131 (1983) 43.
24 H. Seyama and M. Soma, J. Chem. Soc., Farad. Trans., 81 (1985) 485.
25 T. Sugama, The effect of Ca $(OH)_2$-treated ceramic microspheres on the mechanical properties of high temperature lightweight cement composites, Material Research Society Symp. Proc., 1987, Material Research Society, Pittsburgh, PA, Vol. 114, pp. 301–307.
26 D.G. Skipper, F.K. Eaton, F.K. Cartledge and M.E. Tittlebaum, Hazard. Waste Hazard. Mater., 4 (1987) 389.